IJMTST | Volume: 2 | Issue: 03 | March 2016 | ISSN: 2455-3778

Low Current Ripple, High Efficiency Boost Converter with Voltage Multiplier

Kanna Srinivasarao[1] | Yanamala Srikanth[2] | Kuchipudi Manoj[3] | Jampani Kiran[4] | Kamal Kiran Tata[5]

[1,2,3,4]UG Student, Department of Electrical and Electronics Engineering, M.V.R College of Engineering, Vijayawada, A.P, India.
[5]Assistant Professor, Department of Electrical and Electronics Engineering, M.V.R College of Engineering, Vijayawada, A.P, India.

ABSTRACT

An innovative high voltage-gain boost converter, which is made for home inverters contains the combination of switched capacitors and coupled inductors made a voltage multiplier, which is used to increase the output gain of a traditional converter abnormally without using an excessive switching frequency. The setup not only maximizes the efficiency but also eliminates input current ripple almost, which deduces conduction losses and current stress of switches causes to greater extension of input source lifetime. In addition, due to the lossless passive clamp performance, leakage energy is recycled to the output terminal. Hence, large voltage spikes across the main switches are alleviated, and the efficiency is improved. Even the low voltage stress makes the low-voltage-rated MOSFETs be embraced for reductions conduction losses and expense. Ultimately, the prototype circuit with 24-V input voltage, 230-V output, and 1000-W output power is operated to verify its performance. The greatest effectiveness is 97.1 %.

KEYWORDS: *Boost Fly-back Forward, Converter, High Boost Gain, Renewable Systems, Interleaved Voltage, multiplier*

I. INTRODUCTION

Nowadays, renewable energy is increasingly valued and employed worldwide because of energy shortage and environmental contamination [1] – [16].

Renewable energy systems generate low voltage output, and thus, high step-up dc/dc converters have been widely employed in many renewable energy applications such fuel cells, wind power generation, and photovoltaic (PV) systems [17] – [24].

Such systems transform energy from renewable sources into electrical energy and convert low voltage into high voltage via a step-up converter, which can convert energy into electricity using a grid-by-grid inverter or dc micro-grid.

Fig. 1 shows a typical renewable energy system that consists of renewable energy sources, a step-up converter, and an inverter for AC application. The high step-up conversion may require two-stage converters with cascade structure for enough step-up gain, which decreases the efficiency and increases the cost. Thus, a high step-up converter is seen as an important stage in the system because such a system requires a sufficiently high step-up conversion with high efficiency.

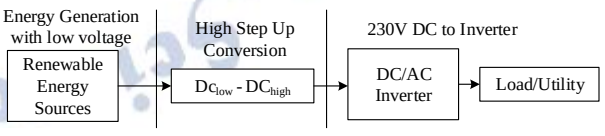

Fig. 1. Typical renewable energy system

Theoretically, conventional step up converters, such as the boost converter and fly-back converter, cannot achieve a high step-up conversion with high efficiency because of the resistances of elements or leakage inductance; also, the voltage stresses are large. Thus, in recent years, many novel high step up converters have been developed [20]–[31].

Despite these advances, high step-up

single-switch converters are unsuitable to operate at heavy load given a large input current ripple, which increases conduction losses.

The conventional interleaved boost converter is an excellent candidate for high-power applications and power factor correction. Unfortunately, the step-up gain is limited, and the voltage stresses on semiconductor components are equal to output voltage.

Hence, based on the aforementioned considerations, modifying a conventional interleaved boost converter for high step-up and high-power application is a suitable approach. To integrate switched capacitors into an interleaved boost converter may make voltage gain reduplicate, but no employment of coupled inductors causes the step-up voltage gain to be limited [32], [33].

Oppositely, to integrate only coupled inductors into an interleaved boost converter may make voltage gain higher and adjustable, but no employment of switched capacitors causes the step-up voltage gain to be ordinary [34], [35].

Thus, the synchronous employment of coupled inductors and switched capacitors is a better concept; moreover, high step-up gain, high efficiency, and low voltage stress are achieved even for high-power applications [36]–[43].

The proposed converter is a conventional interleaved boost converter integrated with a voltage multiplier module, and the voltage multiplier module is composed of switched capacitors and coupled inductors shown in Fig. 2.

The coupled inductors can be designed to extend step-up gain, and the switched capacitors offer extra voltage conversion ratio. In addition, when one of the switches turns off, the energy stored in the magnetizing inductor will transfer via three respective paths; thus, the current distribution not only decreases the conduction losses by lower effective current but also makes currents through some diodes decrease to zero before they turn off, which alleviate diode reverse recovery losses.

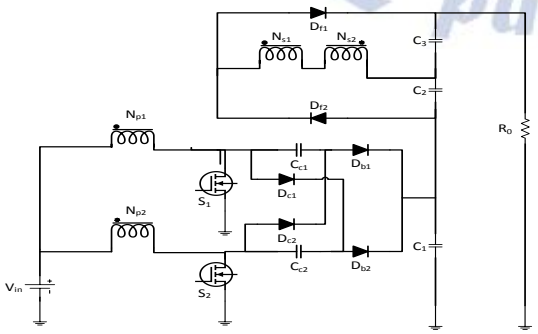

Fig. 2. Proposed high gain converter

The advantages of the proposed converter are as follows.

1) The proposed converter is characterized by low input current ripple and low conduction losses, which increases the lifetime of renewable energy sources and makes it suitable for high-power applications.
2) The converter achieves the high step-up gain that renewable energy systems require.
3) Due to the lossless passive clamp performance, leakage energy is recycled to the output terminal. Hence, large voltage spikes across the main switches are alleviated, and the efficiency is improved.
4) Low cost and high efficiency are achieved by employment of the low-voltage-rated power switch with low $R_{DS(ON)}$;also, the voltage stresses on main switches and diodes are substantially lower than output voltage.
5) The inherent configuration of the proposed converter makes some diodes decrease conduction losses and alleviate diode reverse recovery losses.

II. Operating Principles

The proposed high step-up interleaved converter with a voltage multiplier module is shown in Fig. 2. The voltage multiplier module is composed of two coupled inductors and two switched capacitors and is inserted between a conventional interleaved boost converter to form a modified boost–fly back–forward interleaved structure.

When the switches turn off by turn, the phase whose switch is in OFF state performs as a fly back converter, and the other phase whose switch is in ON state performs as a forward converter.

Primary windings of the coupled inductors with Np turns are employed to decrease input current ripple, and secondary windings of the coupled inductors with Ns turns are connected in series to extend voltage gain. The turn ratios of the coupled inductors are the same. The coupling references of the inductors are denoted by "·" and "∗".

The equivalent circuit of the proposed converter is shown in Fig. 3, where L_{m1} and L_{m2} are the magnetizing inductors; L_{k1} and L_{k2} represent the leakage inductors; L_s represents the series leakage inductors in the secondary side; S1 and S2 denote the power switches; C_{c1} and $C_{c2}$are the switched capacitors; and C_1, C_2, and C_3 are the output capacitors. D_{c1} and D_{c2} are the clamp diodes, D_{b1} and D_{b2} represent the output diodes for boost operation with switched capacitors, D_{f1} and D_{f2}

represent the output diodes for fly back–forward operation, and n is defined as turn ratio N_s/N_p.

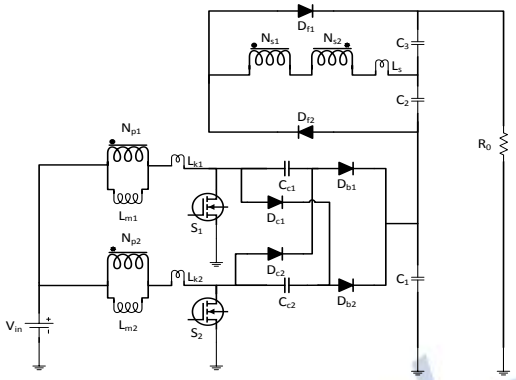

Fig. 3. Equivalent circuit of proposed converter

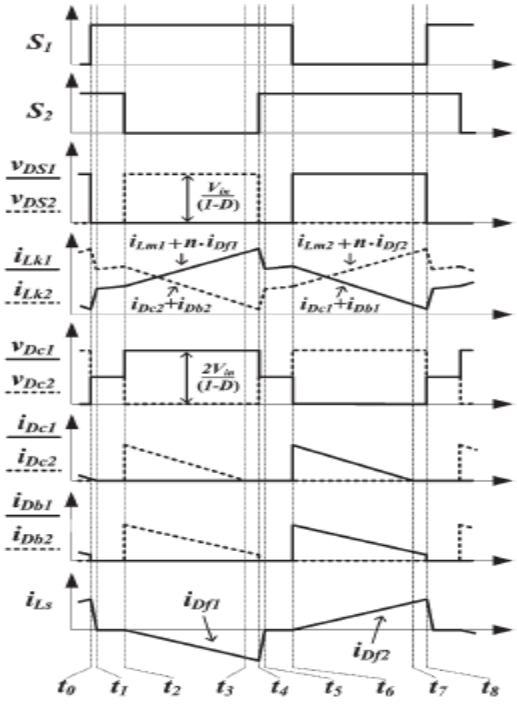

Fig. 4. Steady waveforms of proposed converter

In the circuit analysis, the proposed converter operates in continuous conduction mode (CCM), and the duty cycles of the power switches during steady operation are greater than 0.5 and are interleaved with a 180◦ phase shift. The key steadywaveform in one switching period of the proposed converter contains six modes, which are depicted in Fig. 4 to Fig. 5 shows the topological stages of the circuit.

Mode I [t_0 to t_1]: At t = t_0, the power switch S2 remains in ON state, and the other power switch S1 begins to turn on. The diodes D_{c1}, D_{c2}, D_{b1}, D_{b2}, and D_{f1} are reversed biased, as shown in Fig. 5. The series leakage inductors L_s quickly release the stored energy to the output terminal via fly back–forward diode D_{f2}, and the current through series leakage inductors L_s decreases to zero. Thus, the magnetizing inductor L_{m1} still transfers energy to the secondary side of coupled inductors. The current through leakage inductor L_{k1} increases linearly, and the other current through leakage inductor L_{k2} decreases linearly.

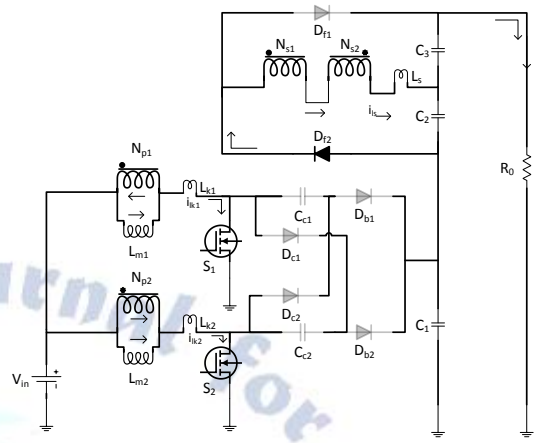

Fig. 5. Mode – I operation

Mode II [t_1 to t_2]: At t = t_1, both of the power switches S1 and S2 remain in ON state, and all diodes are reversed biased, as shown in Fig. 6. Both currents through leakage inductorsL_{k1} and L_{k2} are increased linearly due to charging by input voltage source Vin.

Mode III [$t_2$to t_3]: At t = t_2, the power switch S1 remains in ON state, and the other power switch S2 begins to turn off. The diodes D_{c1}, D_{b1}, and D_{f2} are reversed biased, as shown in Fig. 7. The energy stored in magnetizing inductor L_{m2} transfers to the secondary side of coupled inductors, and the current through series leakage inductors L_s flows to output capacitor C_3 via fly back–forward diodeD_{f1}. The voltage stress on power switch S2 is clamped by clamp capacitor C_{c1} which equals the output voltage of the boost converter. The input voltage source, magnetizing inductor L_{m2}, leakage inductor L_{k2}, and clamp capacitor C_{c2} release energy to the output terminal; thus, V_{C1} obtains a double output voltage of the boost converter.

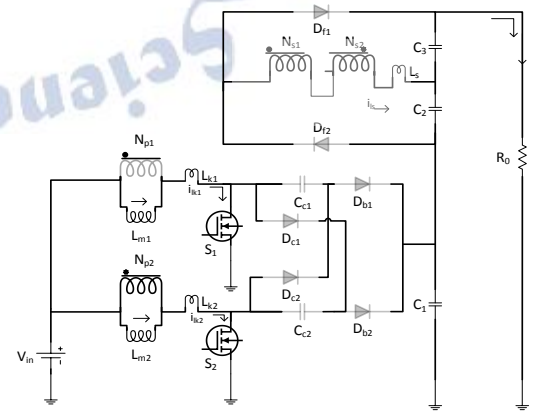

Fig. 6. Mode – II operation

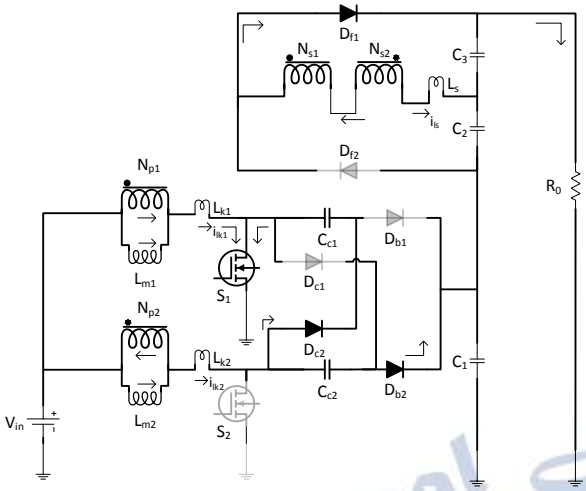

Fig. 7. Mode – III operation

Mode IV [t_3 to t_4]: At t = t_3, the current i_{Dc2} has naturally decreased to zero due to the magnetizing current distribution, and hence, diode reverse recovery losses are alleviated and conduction losses are decreased. Both power switches and all diodes remain in previous states except the clamp diode D_{c2}, as shown in Fig. 8.

Mode V [t_4 to t_5]: At t = t_4, the power switch S1 remains in ON state, and the other power switch S2 begins to turn on. The diodes D_{c1}, D_{c2}, D_{b1}, D_{b2}, and D_{f2} are reversed biased, as shown in Fig. 9. The series leakage inductors Ls quickly release the stored energy to the output terminal via fly back–forward diode D_{f1},and the current through series leakage inductors decrease to zero. Thus, the magnetizing inductor L_{m2} still transfers energy to the secondary side of coupled inductors. The current through leakage inductor L_{k2}increases linearly, and the other current through leakage inductor L_{k1} decreases linearly.

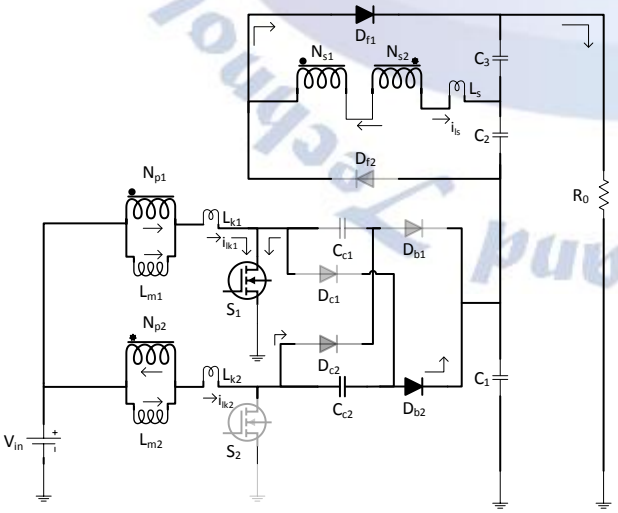

Fig. 8. Mode – IV operation

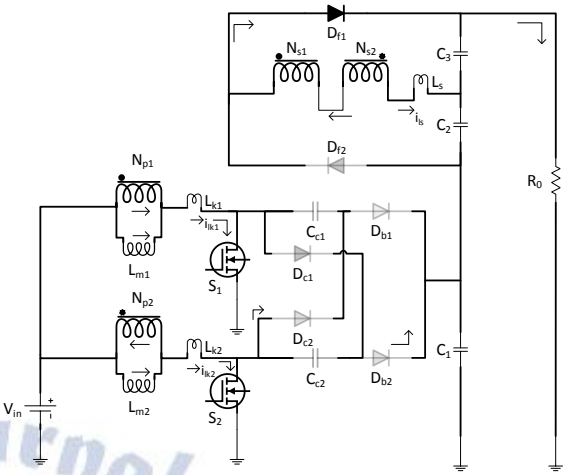

Fig. 9. Mode – V operation

Mode VI [t_5 to t_6]: At t = t_5, both of the power switches S1 and S2 remain in ON state, and all diodes are reversed biased, as shown in Fig. 10. Both currents through leakage inductors L_{k1} and L_{k2} are increased linearly due to charging by input voltage source Vin.

Mode VII [t_6 to t_7]: At t = t_6, the power switch S2 remains in ON state, and the other power switch S1 begins to turn off. The diodes D_{c2}, D_{b2}, and D_{f1} are reversed biased, as shown in Fig. 11. The energy stored in magnetizing inductor Lm1 transfers to the secondary side of coupled inductors, and the current through series leakage inductors flows to output capacitor C_2via fly back–forward diode D_{f2}. The voltage stress on power switch S1 is clamped by clamp capacitor C_{c2} which equals the output voltage of the boost converter. The input voltage source, magnetizing inductor L_{m1}, leakage inductor L_{k1}, and clamp capacitor C_{c1} release energy to the output terminal; thus, V_{C1} obtains double output voltage of the boost converter.

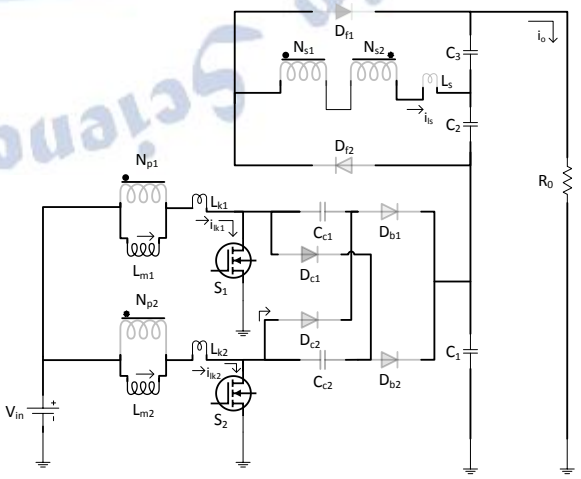

Fig. 10. Mode – VI operation

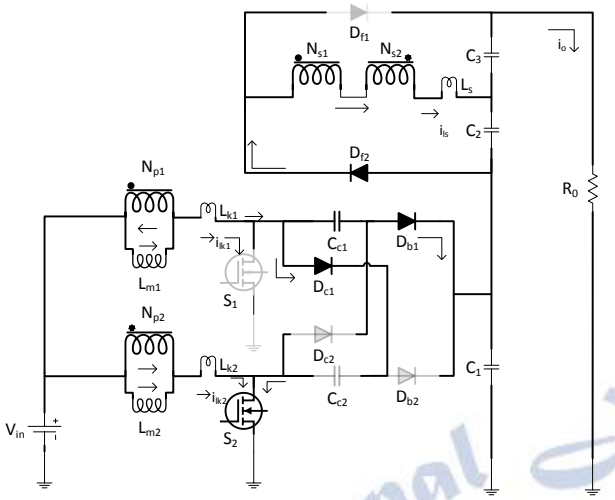

Fig. 11. Mode – VII operation

Mode VIII [t_7 to t_8]: At t = t_7, the current i_{Dc1} has naturally decreased to zero due to the magnetizing current distribution, and hence, diode reverse recovery losses are alleviated and conduction losses are decreased. Both power switches and all diodes remain in previous states except the clamp diode D_{c1}, as shown in Fig. 12.

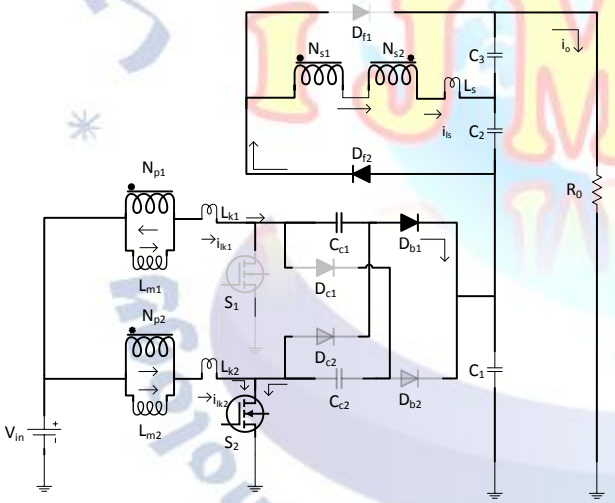

Fig. 12. Mode – VIII operation

III. Steady State Analysis

The transient characteristics of circuitry are disregarded to simplify the circuit performance analysis of the proposed converter in CCM, and some formulated assumptions are as follows.

1) All of the components in the proposed converter are ideal.
2) Leakage inductors L_{k1}, L_{k2}, and L_s are neglected.
3) Voltages on all capacitors are considered to be constant
4) Due to the completely symmetrical interleaved structure, the related components are defined as the corresponding symbols such as $D_{c1}$and D_{c2}defined as D_c.

A. Step-Up Gain

The voltage on clamp capacitor C_c can be regarded as an output voltage of the boost converter; thus, voltage V_{Cc}can be derived from

$$V_{Cc} = \frac{1}{1-D} V_{in} \quad (1)$$

When one of the switches turns off, voltage V_{C1}can obtain a double output voltage of the boost converter derived from

$$V_{C_1} = \frac{1}{1-D} V_{in} + V_{C_c} = \frac{2}{1-D} V_{in} \quad (2)$$

The output filter capacitors C_2 and C_3 are charged by energy transformation from the primary side. When S2 is in ON state and S1 is in OFF state, V_{C2} is equal to the induced voltage of Ns1 plus the induced voltage of Ns2, and when S1 is in ON state and S2 is in OFF state, V_{C3} is also equal to the induced voltage of N_{s1} plus the induced voltage of N_{s2}. Thus, voltages V_{C2} and V_{C3} can be derived from

$$V_{c2} = V_{c3} = n V_{in} \left(1 + \frac{D}{1-d}\right) = \frac{n}{1-D} V_{in} \quad (3)$$

The output voltage can be derived from

$$V_o = V_{c1} + V_{c2} + V_{c3} = \frac{2n+2}{1-D} V_{in} \quad (4)$$

In addition, the voltage gain of the proposed converter is

$$\frac{v_O}{v_{in}} = \frac{2n+2}{1-D} \quad (5)$$

Equation (5) confirms that the proposed converter as a high step-up voltage gain without an extreme duty-cycle. When the duty cycle is merely 0.6, the voltage-gain reaches ten at a turn ratio n of one; the voltage gain reaches 30 at a turn ratio n of five.

B. Voltage Stress on Semiconductor Component

The voltage ripples on the capacitors are ignored to simplify the voltage stress analysis of the components of the proposed converter. The voltage stress on power switch S is clamped and derived from

$$V_{s1} = V_{s2} = \frac{2}{1-D} V_{in} = \frac{1}{2n+2} V_o \quad (6)$$

Equation (6) confirms that low-voltage-rated MOSFET with low RDS(ON) can be adopted for the proposed converter to reduce conduction losses and costs. The voltage stress on the power switch S

accounts for a fourth of output voltage Vo, even if turn ratio n is one. This feature makes the proposed converter suitable for high step-up and high-power applications

The voltage stress on diode D_c is equal to V_{C1}, and the voltage stress on diode D_b is voltage V_{C1} minus voltage V_{Cc}. These voltage stresses can be derived from

$$V_{Dc1} = V_{Dc2} = \frac{2}{1-D}V_{in} = \frac{1}{n+1}V_o \quad (7)$$

$$V_{Db1} = V_{Db2} = V_{c1} - V_{c2} = \frac{1}{1-D}V_{in} = \frac{1}{2n+2}V_o \quad (8)$$

The voltage stress on diode D_b is close to the voltage stress on power switch S. Although the voltage stress on diode D_c is larger, it accounts for only half of output voltage Vo at a turn ratio n of one. The voltage stresses on the diodes are lower as the voltage gain is extended by increasing turn ratio n. The voltage stress on diode D_f equals the V_{C2} plus V_{C3}, which can be derived from

$$V_{Df1} = V_{Df2} = \frac{2n}{1-D}V_{in} = \frac{n}{n+1}V_o \quad (9)$$

Although the voltage stress on the diode D_f increases as the turn ratio n increases, the voltage stress on the diodes D_f is always lower than the output voltage.

The relationship between the voltage stresses on all the semiconductor components and the turn ratio n is illustrated.

C. Analysis of Conduction Losses

Some conduction losses are caused by resistances of semiconductor components and coupled inductors. Thus, all the components in the proposed converter are not assumed to be ideal, except for all the capacitors. Diode reverse recovery problems, core losses, switching losses, and the equivalent series resistance of capacitors are not discussed in this section. The characteristics of leakage inductors are disregarded because of energy recycling.

The equivalent circuit, which includes the conduction losses of coupled inductors and semiconductor components, in which r_{L1} and r_{L2} are the copper resistances of the primary windings of the coupled inductor; r_{Ls} represents the copper resistances of the secondarywindings of the coupled inductors; r_{DS1} and r_{DS2} denote the on-resistances of power switches; V_{Dc1}, V_{Dc2}, V_{Db1}, V_{Db2}, V_{Df1}, and V_{Df2} denote the forward biases of the diodes; and r_{Dc1}, r_{Dc2}, r_{Db1}, r_{Db2}, r_{Df1}, and r_{Df2} are the resistances of the diodes.

Small-ripple approximation was used to calculate conduction losses. Thus, all currents that pass through components were approximated by the dc components. The magnetizing currents and capacitor voltages are assumed to be constant because of the infinite values of magnetizing inductors and capacitors. Finally, through voltage-second balance and capacitor-charge balance, the voltage conversion ratio with conduction losses can be derived from

$$\frac{V_o}{V_{in}} = \frac{\frac{2n+2}{1-D} - \frac{1}{v_{in}}\left(V_{Dc} + V_{Db} + 2V_{Df}\right)}{1 + \frac{(2d-1)\,r_w + r_x}{r_o(1-D)} + \frac{\left[(2D-1)\quad_{r_y}\right] + r_z}{r_o(1-D)}} \quad (10)$$

where

$$r_w = [2(2-D)(n+1) - 1.5]r_{Ds} + 4n(1-D)r_{dc}$$

$$r_x = 2n(2n+1)r_{Ds} + (2n+2)(2nD + 2D - 1)r_L$$

$$r_y = 2(1-2n)r_{Dc} + 0.5r_{Db}$$

$$r_w = 4n^2 r_L + 2\left(r_{Ls} + r_{df}\right)$$

Because the turn ratio n and copper resistances of the secondary windings of the coupled inductors are directly proportional, the copper resistances of the coupled inductors can be expressed as

$$r_{ls} = 2n.r_L$$

Efficiency is expressed as follows:

$$\eta = \frac{1 - \frac{1-D}{V_{in\,(2n+2)}}\left(V_{Dc+VDb+2VDf}\right)}{1 + \frac{(2D-1)r_{w+r_x}}{R_o(1-D)^2} + \frac{\left[(2D-1)r_y\right] + r_z}{R_o.(1-D)}} \quad (11)$$

On the basis of (11), it can be inferred that the efficiency will be higher if the input voltage is considerably higher than the summation of the forward biases of all the diodes or if the resistance of the load is substantially larger than the resistances of coupled inductors and semiconductor components. In addition, the maximal effect for efficiency is duty cycle, and the secondary is the copper resistance of coupled inductors.

D. Performance of Current Distribution

The inherent configuration of the proposed converter makes the energy stored in magnetizing inductors transfer via three respective paths as one of the switches turns off. Thus, the current distribution decreases the conduction losses by lower effective value of current and increases the capacity by lower peak value of current. In addition, if the load is not heavy enough, currents through some diodes decrease to zero before they

turn off, which alleviate diode reverse recovery losses.

Under light-/medium-load condition, the currents through diodes Db and Dc decrease to zero before they turn off. When the load is continuously added, only the current i_{Dc} decreases to zero before diode Dc turns off. Under heavy load, although every current through the diode cannot decrease to zero before the related diode turns off, the reduction of conduction lossesand the increase of capacity still perform well.

E. Consideration for Applications of Renewable Energy Source and Low-Voltage Source

Many low-voltage sources, such as battery, and renewable energy sources, such as solar cell or fuel cell stack, need a high step-up conversion to supply power to high-voltage applications and loads. However, an excellent high step-up converter not only supplies efficient step-up conversion but also should lengthen the lifetime of sources such as battery set and fuel cell stack. Thus, suppression of input current ripple for lengthening the lifetime of sources is also a main design consideration.

The proposed converter can satisfy the aforementioned applications even for high-power load due to the interleaved structure, which makes the power source or battery set discharge smoothly. The proposed converter operated in CCM is even more suitable than that operated in discontinuous conduction mode (DCM) for suppression of input current ripple, because the peak current in DCM is larger. For PV system, maximum power point tracking (MPPT) is an important consideration, and MPPT is implemented by adjusting the duty cycle within a range.

However, the duty cycles of the proposed converter are greater than 0.5 due to the interleaved structure. Thus, if the proposed converter operates in some PV system, which must be satisfied with enough output voltage, duty cycle limitation, and MPPT, the turn ratio n should be set to make the maximum power point easily located in duty cycles greater than 0.5. The turn ratio n can be decreased slightly as a suitable value based on (5), which makes the duty cycle increase. Oppositely, a trade off should be made for practical output power to load between efficiency of the converter and MPPT, because the larger duty cycle causes efficiency to decrease even if copper resistances decreased by smaller turn ratio n.

This section provides important information on characteristic analysis, feature, and consideration, which indicates the relationship among duty cycle, turn ratio, and components The proposed converter for each application can be designed on the basis of selected turn ratios, components, and other considerations.

F. Performance Comparison

For demonstrating the performance of the proposed converter, the proposed converter and the other high step-up interleaved converters introduced in [36] and [40] are compared. The high step-up interleaved converter introduced in [36] is favorable for dc micro-grid applications, and the other high step-up interleaved converter introduced in [40] is suitable as a candidate for high step-up high-power conversion of the PV system. Both of the converters use coupled inductors and switched capacitors to achieve high step-up conversion.

The step-up gain of the proposed converter is the highest, and the voltage stresses on semiconductor devices are the lowest. In addition, the extra winding or core may result in the circuit being costly and bulky. The proposed converter only uses two normal coupled inductors; thus, the cost and degree of difficulty of design are lower. Oppositely, the performances of current sharing and distribution make the reliability, capacity, and efficiency higher

IV. Design and Experiment of Proposed Converter

A 1-kW prototype of the proposed high step-up converter is tested. The electrical specifications are V_{in} = 24 V, V_o = 230 V, and f_s = 40 kHz. The major components have been chosen as follows: Magnetizing inductors L_{m1} and L_{m2} = 133 µH; turn ratio n = 1; power switches S1 and S2 are IRFP4227; diodes D_{c1} and D_{c2} are BYQ28E-200; diodes D_{b1}, D_{b2}, D_{f1}, and D_{f2} are FCF06A-40; capacitors C_{c1}, C_{c2}, C_2, and C_3 = 220 µF; and C_1 = 470 µF.

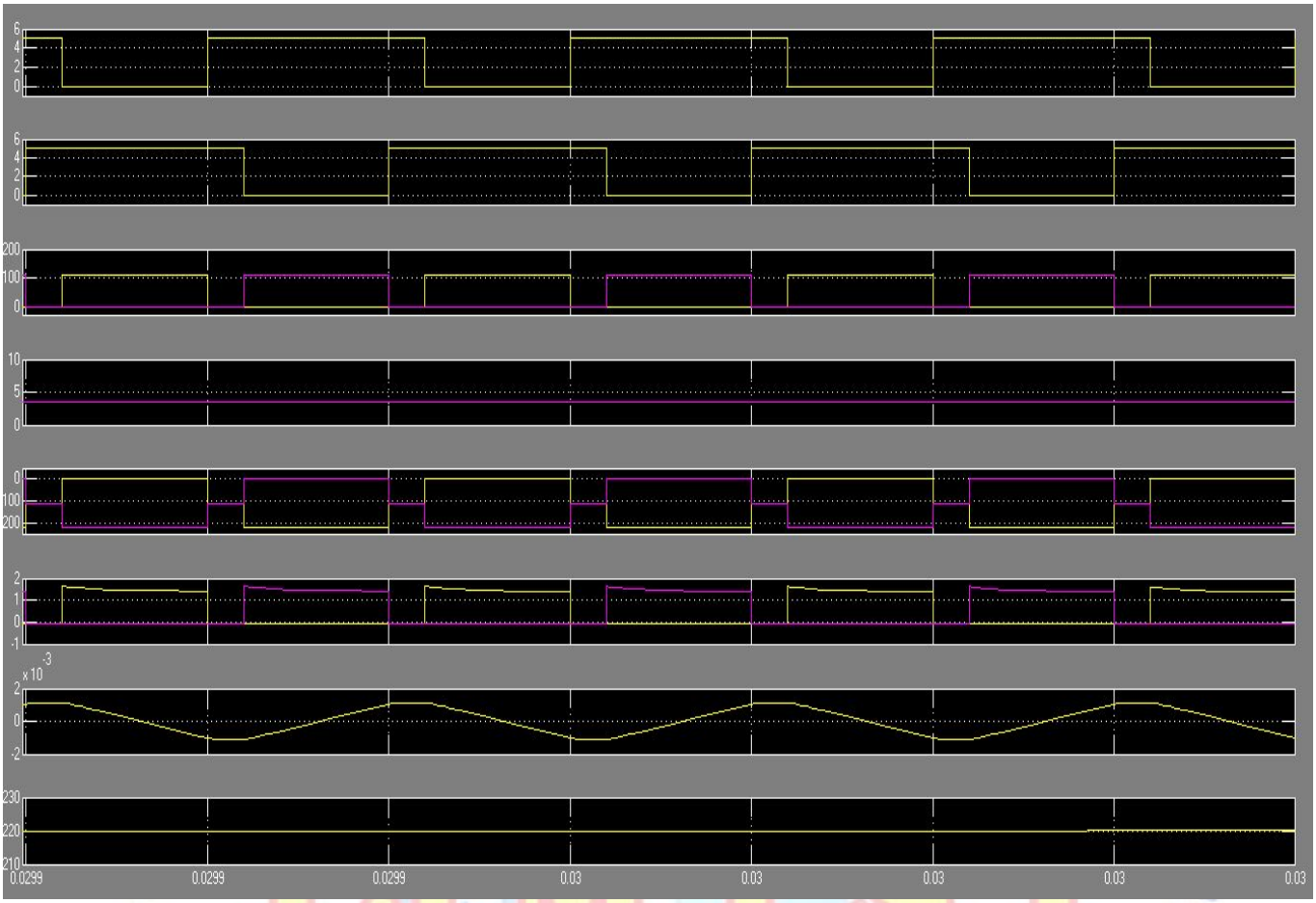

Fig. 13. Simulated waveforms using MATLAB

The design consideration of the proposed converter includes component selection and coupled inductor design, which are based on the analysis presented in the previous section. In theproposed converter, the values of the primary leakage inductors of the coupled inductors are set as close as possible for current sharing performance, and the leakage inductors L_{k1} and L_{k2} are 1.6 μH. Due to the performances of high step-up gain, the turn ratio n can be set as one for the prototype circuit with 24-V input voltage and 230-V output to reduce cost, volume, and conduction loss of the winding. Thus, the copper resistances which affect efficiency much can be decreased.

Fig. 13 shows the simulated waveforms at full load of 1000W. Fig. 13 shows the interleaved pulse width-modulation signalsV_{gs1} and V_{gs2}, as well as the voltage stresses on the power switches. V_{DS1} and V_{DS2} are clamped at 100 V, which is much lower than the output voltage. Fig. 13 shows the voltage stresses on clamp diodes and the current through clamp diodes. The voltage stresses V_{Dc1} and V_{Dc2} are doubles of V_{DS1} and V_{DS2}. The currents i_{Dc1} and i_{Dc2} decrease to zero before they turn off, which alleviate diode reverse recovery losses.

Fig. 13 shows the waveform of v_{Db1}, v_{Db2}, i_{Db1}, and i_{Db2}.The voltage stresses v_{Db1} and v_{Db2} are equal to the voltage stresses on power switches.

Fig. 13 shows the waveform of v_{Df1}, v_{Df2}, and i_{Ls}. The voltage stresses v_{Df1} and v_{Df2} are equal to v_{Dc1} and v_{Dc2} because the turn ratio n is set as one, and the ringing characteristics are caused by the series leakage inductors L_s. Fig. 13 shows the output voltage and voltages on output capacitors. The output voltage V_o is 380 V. Because the turn ratio n is set as one, the voltages V_{C2} and V_{C3} are half of V_{C1}. From experimental results, it can be proved that the voltages on output capacitors are in accordance with those of steady-state analysis, and all of the measured voltage stresses are corresponding to those, which are illustrated by theoretical analysis. Fig. 13 shows the input currentI_{in} and each current through the primary leakage inductor, which demonstrates the performance of current sharing.

The maximum efficiency is 97.1% at Po = 400 W. At full load of 1 kW, the conversion efficiency is about 96.4%.

V. Conclusion

This paper has presented the theoretical analysis of steady state, related consideration, simulation results, and experimental results for the proposed converter. The proposed converter has successfully implemented an efficient high step-up conversion through the voltage multiplier module. The interleaved structure reduces the input current ripple and distributes the current through each component. In addition, the lossless passive clamp function recycles the leakage energy and constrains a large voltage spike across the power switch. Meanwhile, the voltage stress on the power switch is restricted and much lower than the output voltage (380 V). Furthermore, the full-load efficiency is 96.4% at P_o = 1000 W, and the highest efficiency is 97.1% at P_o = 400 W. Thus, the proposed converter is suitable for high-power or renewable energy applications that need high step-up conversion.

References

[1] T. Bialasiewicz, "Renewable energy systems with photovoltaic power generators: Operation and modeling," *IEEE Trans. Ind. Electron.*, vol. 55, no. 7, pp. 2752–2758, Jul. 2008.

[2] T. Kefalas and A. Kladas, "Analysis of transformers working under heavily saturated conditions in grid-connected renewable energy systems," *IEEE Trans. Ind. Electron.*, vol. 59, no. 5, pp. 2342–2350, May 2012.

[3] Y. Xiong, X. Cheng, Z. J. Shen, C. Mi, H. Wu, and V. K. Garg, "Prognostic and warning system for power-electronic modules in electric, hybrid electric, and fuel-cell vehicles," *IEEE Trans. Ind. Electron.*, vol. 55, no. 6, pp. 2268–2276, Jun. 2008.

[4] A. K. Rathore, A. K. S. Bhat, and R. Oruganti, "Analysis, design and experimental results of wide range ZVS active-clamped L–L type current fed DC/DC converter for fuel cells to utility interface," *IEEE Trans. Ind.Electron.*, vol. 59, no. 1, pp. 473–485, Jan. 2012.

[5] T. Zhou and B. Francois, "Energy management and power control of a hybrid active wind generator for distributed power generation and grid integration," *IEEE Trans. Ind. Electron.*, vol. 58, no. 1, pp. 95–104, Jan. 2011.

[6] N. Denniston, A. M. Massoud, S. Ahmed, and P. N. Enjeti, "Multiple module high-gain high-voltage DC–DC transformers for offshore wind energy systems," *IEEE Trans. Ind. Electron.*, vol. 58, no. 5, pp. 1877– 1886, May 2011.

[7] H. Tao, J. L. Duarte, andM. A.M. Hendrix, "Line-interactive UPS using a fuel cell as the primary source," *IEEE Trans. Ind. Electron.*, vol. 55, no. 8, pp. 3012–3021, Aug. 2008.

[8] K. Jin, X. Ruan, M. Yan, and M. Xu, "A hybrid fuel cell system," *IEEE Trans. Ind. Electron.*, vol. 56, no. 4, pp. 1212–1222, Apr. 2009.

[9] A. I. Bratcu, I. Munteanu, S. Bacha, D. Picault, and B. Raison, "Cascaded DC–DC converter photovoltaic systems: Power optimization issues," *IEEE Trans. Ind. Electron.*, vol. 58, no. 2, pp. 403–411, Feb. 2011.

[10] R. J. Wai, W. H. Wang, and C. Y. Lin, "High-performance stand-alone photovoltaic generation system," *IEEE Trans. Ind. Electron.*, vol. 55, no. 1, pp. 240–250, Jan. 2008.

[11] R. J. Wai and W. H. Wang, "Grid-connected photovoltaic generation system," *IEEE Trans. Circuits Syst. I, Reg. Papers*, vol. 55, no. 3, pp. 953–964, Apr. 2008.

[12] L. Gao, R. A. Dougal, S. Liu, and A. P. Iotova, "Parallel-connected solar PV system to address partial and rapidly fluctuating shadow conditions," *IEEE Trans. Ind. Electron.*, vol. 56, no. 5, pp. 1548–1556, May 2009.

[13] B. Yang, W. Li, Y. Zhao, and X. He, "Design and analysis of a grid connected photovoltaic power system," *IEEE Trans. Power Electron.*, vol. 25, no. 4, pp. 992–1000, Apr. 2010.

[14] W. Li and X. He, "Review of non-isolated high-step-up DC/DC converters in photovoltaic grid-connected applications," *IEEE Trans. Ind. Electron.*, vol. 58, no. 4, pp. 1239–1250, Apr. 2011.

[15] C. T. Pan and C. M. Lai, "A high-efficiency high step-up converter with low switch voltage stress for fuel-cell system applications," *IEEE Trans.Ind. Electron.*, vol. 57, no. 6, pp. 1998–2006, Jun. 2010.

[16] R. J.Wai and R. Y. Duan, "High step-up converter with coupled-inductor," *IEEE Trans. Power Electron.*, vol. 20, no. 5, pp. 1025–1035, Sep. 2005.

[17] S. K. Changchien, T. J. Liang, J. F. Chen, and L. S. Yang, "Novel highstep-up DC–DC converter for fuel cell energy conversion system," *IEEE Trans. Ind. Electron.*, vol. 57, no. 6, pp. 2007–2017, Jun. 2010.

[18] Y. P. Hsieh, J. F. Chen, T. J. Liang, and L. S. Yang, "Novel high step upDC–DC converter with coupled-inductor and switched-capacitor techniques for a sustainable energy system," *IEEE Trans. Power Electron.*, vol. 26, no. 12, pp. 3481–3490, Dec. 2011.

[19] Y.-P. Hsieh, J.-F. Chen, T.-J. Liang, and L. S. Yang, "A novel high step-up DC–DC converter for a micro grid system," *IEEE Trans. Power Electron.*, vol. 26, no. 4, pp. 1127–1136, Apr. 2011.

[20] C. Evangelista, P. Puleston, F. Valenciaga, and L.M. Fridman, "Lyapunov designed super-twisting sliding mode control for wind energy conversion optimization," *IEEE Trans. Ind. Electron.*, vol. 60, no. 2, pp. 538–545, Feb. 2013.

[21] R. Li and D. Xu, "Parallel operation of full power converters inpermanent-magnet direct-drive wind power generation system," *IEEETrans. Ind. Electron.*, vol. 60, no. 4, pp. 1619–1629, Apr. 2013.

[22] L. Barote, C. Marinescu, and M. N. Cirstea, "Control structure for single phase stand-alone wind-based

energy sources," *IEEE Trans. Ind. Electron.*, vol. 60, no. 2, pp. 764–772, Feb. 2013.

[23] Z. Song, C. Xia, and T. Liu, "Predictive current control of three-phasegrid-connected converters with constant switching frequency for wind nergy systems," *IEEE Trans. Ind. Electron.*, vol. 60, no. 6, pp. 2451– 2464, Jun. 2013.

[24] S. M. Chen, T. J. Liang, L. S. Yang, and J. F. Chen, "A safety enhanced, high step-up DC–DC converter for AC photovoltaic module application," *IEEE Trans. Power Electron.*, vol. 27, no. 4, pp. 1809–1817, Apr. 2012.

[25] Q. Zhao and F. C. Lee, "High-efficiency, high step-up DC–DC converters," *IEEE Trans. Power Electron.*, vol. 18, no. 1, pp. 65–73, Jan. 2003.

[26] K. C. Tseng and T. J. Liang, "Novel high-efficiency step-up converter," *Proc. Inst. Elect. Eng.—Elect. Power Appl.*, vol. 151, no. 2, pp. 182–190, Mar. 2004.

[27] T. J. Liang and K. C. Tseng, "Analysis of integrated boost–fly-back step up converter," *Proc. Inst. Elect. Eng.—Elect. Power Appl.*, vol. 152, no. 2, pp. 217–225, Mar. 2005.

[28] F. L. Luo, "Six self-lift DC–DC converters, voltage lift technique," *IEEE Trans. Ind. Electron.*, vol. 48, no. 6, pp. 1268–1272, Dec. 2001.

[29] L. S. Yang, T. J. Liang, and J. F. Chen, "Transformerless DC–DC converters with high step-up voltage gain," *IEEE Trans. Ind. Electron.*, vol. 56, no. 8, pp. 3144–3152, Aug. 2009.

[30] R. J. Wai, C. Y. Lin, R. Y. Duan, and Y. R. Chang, "High-efficiency DC–DC converter with high voltage gain and reduced switch stress," *IEEE Trans. Ind. Electron.*, vol. 54, no. 1, pp. 354–364, Feb. 2007.

[31] Y. P. Hsieh, J. F. Chen, T. J. Liang, and L. S. Yang, "Novel high step-up DC–DC converter for distributed generation system," *IEEE Trans. Ind.Electron.*, vol. 60, no. 4, pp. 1473–1482, Apr. 2013.

[32] Y. Jang and M. M. Jovanovic, "Interleaved boost converter with intrinsic voltage-doubler characteristic for universal-line PFC front end," *IEEETrans. Power Electron.*, vol. 22, no. 4, pp. 1394–1401, Jul. 2007.

[33] M. Prudente, L. L. Pfitscher, G. Emmendoerfer, E. F. Romaneli, andR. Gules, "Voltage multiplier cells applied to non-isolated DC–DC converters,"*IEEE Trans. Power Electron.*, vol. 23, no. 2, pp. 871–887, Mar. 2008.

[34] W. Li and X. He, "An interleaved winding-coupled boost converter with passive lossless clamp circuits," *IEEE Trans. Power Electron.*, vol. 22, no. 4, pp. 1499–1507, Jul. 2007.

[35] G. A. L. Henn, R. N. A. L. Silva, P. P. Praca, L. H. S. C. Barreto, and D. S. Oliveira, Jr., "Interleaved-boost converter with high voltage gain," *IEEE Trans. Power Electron.*, vol. 25, no. 11, pp. 2753–2761, Nov. 2010.

[36] C. M. Lai, C. T. Pan, and M. C. Cheng, "High-efficiency modular high step-up interleaved boost converter for DC-microgrid applications," *IEEETrans. Ind. Appl.*, vol. 48, no. 1, pp. 161–171, Jan./Feb. 2012.

[37] D. Wang, X. He, and J. Shi, "Design and analysis of an interleaved fly-back–forward boost converter with the current auto balance characteristic," *IEEE Trans. Power Electron.*, vol. 25, no. 2, pp. 489–498, Feb. 2010.

[38] K. C. Tseng, C. C. Huang, and W. Y. Shih, "A high step-up converter with a voltage multiplier module for a photovoltaic system," *IEEE Trans.Power Electron.*, vol. 28, no. 6, pp. 3047–3057, Jun. 2013.

[39] W. Li, Y. Zhao, Y. Deng, and X. He, "Interleaved converter with voltage multiplier cell for high step-up and high-efficiency conversion," *IEEETrans. Power Electron.*, vol. 25, no. 9, pp. 2397–2408, Sep. 2010.

[40] W. Li, Y. Zhao, J. Wu, and X. He, "Interleaved high step-up converter with winding-cross-coupled inductors and voltage multiplier cells," *IEEETrans. Power Electron.*, vol. 27, no. 1, pp. 133–143, Jan. 2012.

[41] W. Li,W. Li, X. He, D. Xu, and B.Wu, "General derivation law of non-isolated high-step-up interleaved converters with built-in transformer," *IEEETrans. Ind. Electron.*, vol. 59, no. 3, pp. 1650–1661, Mar. 2012.

[42] W. Li, X. Xiang, C. Li, W. Li, and X. He, "Interleaved high step-up ZVT converter with built-in transformer voltage doubler cell for distributed PV generation system," *IEEE Trans. Ind. Electron.*, vol. 28, no. 1, pp. 300– 313, Jan. 2013.

[43] Y. Zhao, X. Xiang, W. Li, X. He, and C. Xia, "Advanced symmetrical voltage quadrupler rectifiers for high step-up and high output-voltage converters," *IEEE Trans. Power Electron.*, vol. 28, no. 4, pp. 1622–1631, Apr. 2013.